Deficiency in the membrane protein Tmbim3a/Grinaa initiates cold-induced ER stress and cell death by activating an intrinsic apoptotic pathway in zebrafish

Received for publication, January 31, 2019, and in revised form, May 31, 2019 Published, Papers in Press, June 6, 2019, DOI 10.1074/jbc.RA119.007813

Kai Chen[‡§], **Xixi Li**[‡§], **Guili Song**[‡], **Tong Zhou**[‡§], **Yong Long**[‡], **Qing Li**[‡], **Shan Zhong**[¶], **and Zongbin Cui**[‡‖1]

From the [‡]*State Key Laboratory of Freshwater Ecology and Biotechnology, Institute of Hydrobiology, Chinese Academy of Sciences, Hubei, Wuhan 430072, China, the* [§]*University of Chinese Academy of Sciences, Beijing 100049, China, the* [¶]*Department of Genetics, Wuhan University, Wuhan, Hubei 430071, China, and the* [‖]*Innovative Academy of Seed Design, Chinese Academy of Sciences, Beijing 100101, China*

Edited by Xiao-Fan Wang

Most members of the family of proteins containing a transmembrane BAX inhibitor motif (TMBIM) have anti-apoptotic activity, but their *in vivo* functions and intracellular mechanisms remain obscure. Here, we report that zebrafish Tmbim3a/Grinaa functions in the prevention of cold-induced endoplasmic reticulum (ER) stress and apoptosis. Using a gene-trapping approach, we obtained a mutant zebrafish line in which the expression of the *tmbim3a/grinaa* gene is disrupted by a Tol2 transposon insertion. Homozygous *tmbim3a/grinaa* mutant larvae exhibited time-dependently increased mortality and apoptosis under cold exposure (at 16 °C). Mechanistically, using immunofluorescence, fluorescence-based assessments of intracellular/mitochondrial Ca^{2+} levels, mitochondrial membrane potential measurements, and Ca^{2+}-ATPase assays, we found that cold exposure suppresses sarcoplasmic/ER Ca^{2+}-ATPase (SERCA) activity and induces the unfolded protein response (UPR) and ER stress. We also found that the cold-induced ER stress is increased in homozygous *tmbim3a/grinaa* mutant embryos. The cold-stress hypersensitivity of the *tmbim3a/grinaa* mutants was tightly associated with disrupted intracellular Ca^{2+} homeostasis, followed by mitochondrial Ca^{2+} overload and cytochrome *c* release, leading to the activation of caspase 9– and caspase-3–mediated intrinsic apoptotic pathways. Treatment of zebrafish larvae with the intracellular Ca^{2+} chelator 1,2-bis(2-aminophenoxy)ethane-*N*,*N*,*N*′,*N*′-tetraacetate-acetoxymethyl ester (BAPTA-AM) or with 2-aminoethoxydiphenyl borate (2-APB), an inhibitor of the calcium-releasing protein inositol 1,4,5-trisphosphate receptor (IP_3R), alleviated cold-induced cell death. Together, these findings unveil a key role of Tmbim3a/Grinaa in relieving cold-induced ER stress and in protecting cells against caspase 9– and caspase 3–mediated apoptosis during zebrafish development.

Apoptosis is a conserved biological process essential for embryogenesis, tissue homeostasis, and responses to pathogens and other stresses in vertebrates (1). Many regulators and effectors have been identified to control the death of cells in animals, and their abnormal expression can lead to a variety of diseases, including cancer, autoimmunity, and degenerative disorders (2). During the past two decades, a number of transmembrane BAX inhibitor motif–containing (TMBIM) family proteins, including TMBIM1–TMBIM6, were identified to control cell death (3). TMBIM family proteins are highly conserved in mammals, zebrafish, and flies, with homologs present even in species where no BCL-2 family members have been identified, including plants, yeast, and many viruses (4). Thus, the control of cell death by TMBIM family proteins may represent a more fundamental and highly conserved pathway in lower organisms (5). However, the biological and physiological functions of most TMBIM proteins remain poorly characterized due to the lack of *in vivo* verification.

TMBIM3/Grina is specifically localized at the membranes of the endoplasmic reticulum (ER)[2] and Golgi compartment (3, 6). Silencing of TMBIM3/GRINA expression does not induce spontaneous cell death in mammalian fibroblasts (3), and the *tmbim3/grina*-deficient mouse did not have an obvious phenotype (6). However, ectopic expression of mouse TMBIM3/GRINA specifically reduced cell death induced by several ER stress agents, but not by other agents that activate both intrinsic and extrinsic apoptosis (3). Moreover, TMBIM3/GRINA and TMBIM6/BI-1 can form a protein complex, and their double mutants are lethal and extremely susceptible to pharmacological ER stress (3). Therefore, TMBIM3/GRINA and TMBIM6/BI-1 appear to have complementary and redundant activities in protection against ER stress–induced cell death.

Temperature is one of environmental factors that determine nearly all life activities of fishes, including embryonic develop-

This work was supported by Science Fund for the Creative Research Group of the National Natural Science Foundation of China Grant 31721005 and National Natural Science Foundation of China Grants 31872554, 31572610, and 31772836. The authors declare that they have no conflicts of interest with the contents of this article.

This article contains Tables S1 and S2 and Figs. S1–S7.

[1] To whom correspondence should be addressed: Institute of Hydrobiology, Chinese Academy of Sciences, Hubei, Wuhan 430072, China. Tel./Fax: 0086-27-68780090; E-mail: zbcui@ihb.ac.cn.

[2] The abbreviations used are: ER, endoplasmic reticulum; qPCR, real-time quantitative PCR; UPR, unfolded protein response; hpf, h post-fertilization; 4-PBA, 4-phenyl butyric acid; MMP, mitochondrial membrane potential; CCCP, carbonyl cyanide 3-chlorophenylhydrazone; CsA, cyclosporin A; IP_3R, inositol 1,4,5-trisphosphate receptor; BAPTA-AM, 1,2-bis(2-aminophenoxy)ethane-*N*,*N*,*N*′,*N*′-tetraacetate-acetoxymethyl ester; 2-APB, 2-aminoethoxydiphenyl borate; WISH, whole-mount *in situ* hybridization; DAPI, 4′,6-diamidino-2-phenylindole; RFP, red fluorescent protein.

ment, growth, reproduction, metabolism, behavior, and distribution. Temperature approaching to or beyond the low temperature limit of fishes can severely disturb their physiological, biochemical, and metabolic functions as well as behaviors, which ultimately results in mortality. It is reported that cold-induced apoptosis in cultured hepatocytes and liver endothelial cells was mediated by reactive oxygen species (7). A large number of differentially expressed genes in previous studies were identified from fish models under cold exposure and uncovered key biological processes and signaling pathways responding to cold stress (8–10). In addition to major cold responses, such as antioxidant response, increased mitochondrial function, and membrane compositional changes, transcriptomic analysis of liver in gilthead sea bream has revealed a key role of unfolded protein response (UPR) to ER stress during short- and long-term exposure to cold (11). However, molecular mechanisms controlling the cell death and individual mortality of fish under cold exposure remain largely unclear.

Zebrafish is widely used as a research model for multiple disciplines, including developmental biology, genetics, physiology, toxicology, and environmental genomics (9). Two TMBIM3-like proteins, Tmbim3a/Grinaa and Tmbim3b/Grinab, can be found in the genome of zebrafish. The transcription of the *tmbim3a*/*grinaa* gene in cold-acclimated zebrafish was significantly up-regulated by RNA-Seq analysis of our previous study (10). Knockdown of Tmbim3b/Grinab in zebrafish using morpholino led to enhanced apoptosis during development of the nervous system (3). However, functions and mechanisms of Tmbim3/Grina in zebrafish remain largely unknown.

In this study, we generated a *tmbim3a*/*grinaa* mutant through a gene-trapping approach. Homozygous *tmbim3a*/*grinaa* mutants are viable and fertile, but their larvae exhibited an increased individual mortality and apoptosis under cold stress. We further dissected Tmbim3a/Grinaa functions in ER-Ca^{2+} homeostasis and ER stress–mediated intracellular signaling for the control of apoptosis in developing embryos of zebrafish exposed to low temperature.

Results

Characterization of tmbim3a/grinaa mutants

In a screening for insertion mutants through a Tol2 transposon–mediated gene-trapping approach (12), we identified a zebrafish line that carries a Tol2 transposon in the second intron of the *tmbim3a*/*grinaa* gene through PCR-based genome walking assays (Fig. 1*A*). Homozygous (*Homo*) and heterozygous (*Hetero*) mutants can be detected with two PCR primer sets, f/r1 and f/r2, respectively (Fig. 1*B*). Tmbim3a/Grinaa of zebrafish (Z-grinaa) shares a higher degree of amino acid sequence similarity with those of human GRINA and mouse Grina than Tmbim3b/Grinab (Z-grinab) (Fig. S1). To generate homozygous mutants, the founder fish (F0) was crossed with WT fish to produce F1 offspring, and 29.2% of F1 fish carried the Tol2 transposon in their genome. The positive F1 fish were then mated with WT fish to obtain F2 offspring. PCR analysis indicated that the positive rate of F2 fish was 46.1% (Table S2). Moreover, 21.2% (42 of 198) of F3 offspring that were produced by the intercross of positive F2 individuals were homozygous mutants. These data fit well with the standard Mendelian inheritance ratio (50 and 25% in F2 and F3 offspring, respectively), suggesting that the Tol2 transposon in this fish line was integrated into a single chromosomal locus.

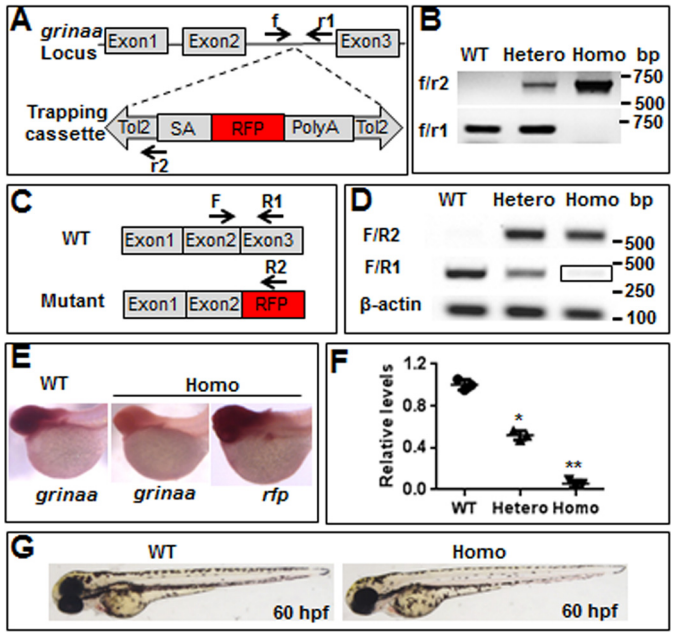

Figure 1. Generation of zebrafish *tmbim3a*/*grinaa* mutants. *A*, the Tol2 transposon element was inserted into the second intron of the *tmbim3a*/*grinaa* gene. The positions of PCR primers (f, r1, and r2) for insertion site analysis are shown. *B*, identification of WT, heterozygous (*Hetero*) and homozygous (*Homo*) mutants, and mutants with PCR primers f, r1, and r2. *C*, predicted WT mature transcript and *tmbim3a*/*grinaa*-RFP fusion transcripts. The positions of PCR primers (F, R1, and R2) for transcript analysis are shown. *D*, transcript analysis with PCR primers in WT, heterozygous, and homozygous embryos at 60 hpf. *E*, detection of the expression patterns of *tmbim3a*/*grinaa* or *rfp* in WT and homozygous embryos at 48 hpf with WISH. *F*, qPCR analysis of *tmbim3a*/*grinaa* in WT, heterozygous, and homozygous embryos at 60 hpf. β-Actin was used as an internal control. *, $p < 0.05$; **, $p < 0.01$. *G*, morphological phenotypes of WT and homozygous embryos at 60 hpf.

The insertion of the Tol2 transposon into the *tmbim3a*/*grinaa* locus would produce a fused transcript containing the second exon of *tmbim3a*/*grinaa* and the RFP coding sequence in *tmbim3a*/*grinaa* mutants (Fig. 1*C*). Indeed, fused transcripts were detected only in heterozygous and homozygous mutants using a primer set F/R2 for RT-PCR, and the transcription of endogenous *tmbim3a*/*grinaa* gene was markedly blocked by the Tol2 insertion in heterozygous and homozygous mutants when detected with a primer set F/R1 (Fig. 1*D*) and whole-mount *in situ* hybridization (Fig. 1*E*). qPCR indicated that transcriptional levels of endogenous *tmbim3a*/*grinaa* gene in heterozygous and homozygous embryos at 60 h post-fertilization (hpf) decreased to 51.8 and 5.3% of that in WT embryos, respectively (Fig. 1*F*). However, homozygous embryos at 60 hpf were morphologically the same as the WT embryos (Fig. 1*G*). Thus, homozygous *tmbim3a*/*grinaa* mutants are viable and fertile under standard rearing conditions and can be used as a loss-of-function model to study physiological and cellular roles of endogenous TMBIM3a/Grinaa.

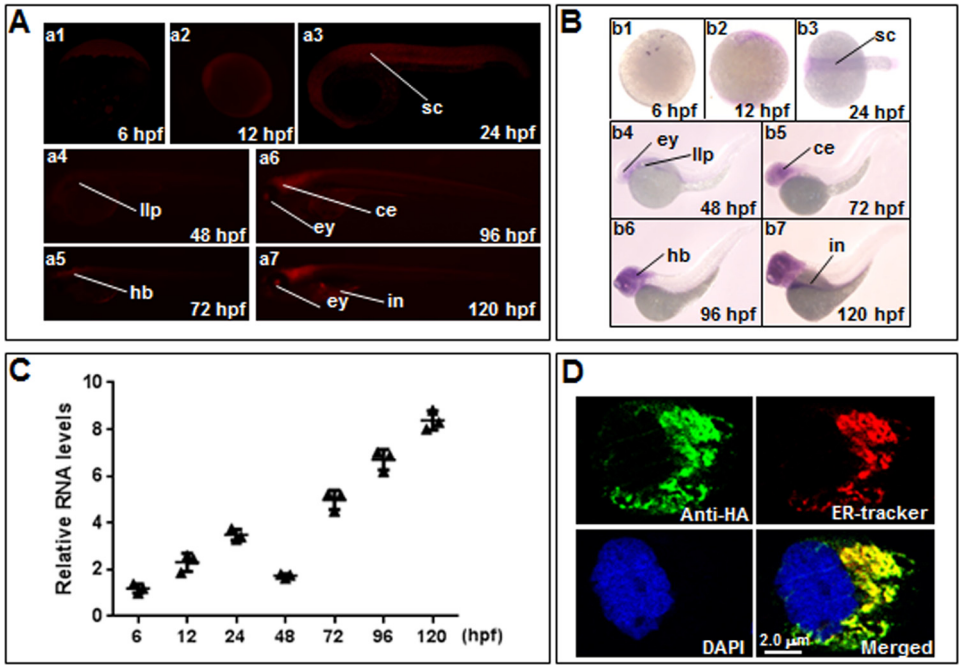

Figure 2. Expression patterns and intracellular localization of zebrafish Tmbim3a/Grinaa. *A*, RFP expression patterns in developing homozygous mutant embryos at the indicated stages. *sc*, spinal cord; *ey*, eyes; *llp*, lateral line primordium; *ce*, cerebellum; *hb*, hindbrain; *in*, intestine. *B*, spatiotemporal expression patterns of *tmbim3a*/*grinaa* in WT embryos at the indicated stages were analyzed with WISH. *C*, transcriptional levels of zebrafish *tmbim3a*/*grinaa* in developing embryos. Fifty embryos at the indicated stages were pooled for total RNA extraction and subjected to qPCR analysis. Values are given as mean ± S.D. (*error bars*), $n = 3$. *D*, ZF4 cells were transfected with HA-tagged Tmbim3a/Grinaa-expressing vectors. Subcellular localization of zebrafish Tmbim3a/Grinaa was evaluated by co-staining with immunofluorescence (12), ER tracker (*red*), and DAPI (*blue* for nucleus), followed by imaging with confocal microscopy.

Embryonic and subcellular distributions of Tmbim3a/Grinaa in zebrafish

Spatiotemporal expression patterns of RFP in heterozygous *tmbim3a*/*grinaa* mutant embryos were imaged. As shown in Fig. 2*A*, RFP was ubiquitously distributed in developing embryos before 12 hpf (Fig. 2*A*, *a1* and *a2*) and prominently expressed in the spinal cord (*sc*) at 24 hpf (Fig. 2*A*, *a3*). Relatively high levels of RFP were observed in the lateral line primordium (*llp*), hindbrain (*hb*), cerebellum (*ce*), and eyes (*ey*) of embryos at 48–96 hpf (Fig. 2*A*, *a4*–*a6*). RFP appeared in the intestine (*in*) of embryos at 120 hpf (Fig. 2*A*, *a7*). These RFP expression patterns in heterozygous *tmbim3a*/*grinaa* mutant embryos were almost identical to the spatiotemporal expression patterns of endogenous *tmbim3a*/*grinaa* gene in developing WT embryos examined with whole-mount *in situ* hybridization (WISH) assays (Fig. 2*B*). Moreover, *tmbim3a*/*grinaa* mRNA was detectable at variable levels in embryos at 6–120 hpf (Fig. 2*C*). These data indicate that the RFP expression in *tmbim3a*/*grinaa* mutants is precisely controlled by the *tmbim3a*/*grinaa* promoter.

The subcellular distribution of Tmbim3a/Grinaa in ZF4 cells (zebrafish embryonic fibroblast–like cell line) was further detected with immunofluorescence staining. We found that HA-tagged TMBIM3a/Grinaa was co-localized well with an ER tracker (Fig. 2*D*), suggesting that physiological and cellular functions of zebrafish TMBIM3a/Grinaa are likely associated with the ER.

Tmbim3a/Grinaa has protective effects on the survival of developing embryos under cold stress

Because homozygous *tmbim3a*/*grinaa* mutants are viable and fertile, we explored the effects of cold stress on developing zebrafish embryos by examination of the death and hatching rates of developing embryos. We have previously found that WT zebrafish larvae exposed to 16–18 °C developed cold acclimation response and showed no mortality during the acclimation process (13). Thus, we dissected the function of Tmbim3a/Grinaa under cold stress at 16 °C. As shown in Fig. 3*A*, death rates of homozygous *tmbim3a*/*grinaa* mutant embryos exposed to 16 °C for 36–240 h markedly increased from 6 to 92% compared with those of WT embryos from 2 to 8%, and average hatching rates of homozygous and WT embryos were 28 and 96%, respectively (Fig. 3*B*). These results suggest that Tmbim3a/Grinaa plays a protective role during zebrafish embryogenesis under cold condition. This notion was supported by the significant induction of endogenous *tmbim3a*/*grinaa* expression in WT larvae and *rfp* expression in homozygous mutants at 16 °C (Fig. 3*C*) as well as the induced RFP fluorescence intensity in homozygous mutant embryos at 16 °C (Fig. 3*D*).

Because the swimming behavior of zebrafish has been used as an indicator for cold tolerance (14), zebrafish larvae at 96 hpf were exposed to 16 °C for 24 h and then transferred to a Zebraview system observation chamber to record the spontaneous swimming behavior for 2 h. The moving paths at different intervals were recorded and analyzed according to the intensities of three classes of swimming activity: slow (*black*), mild (*green*),

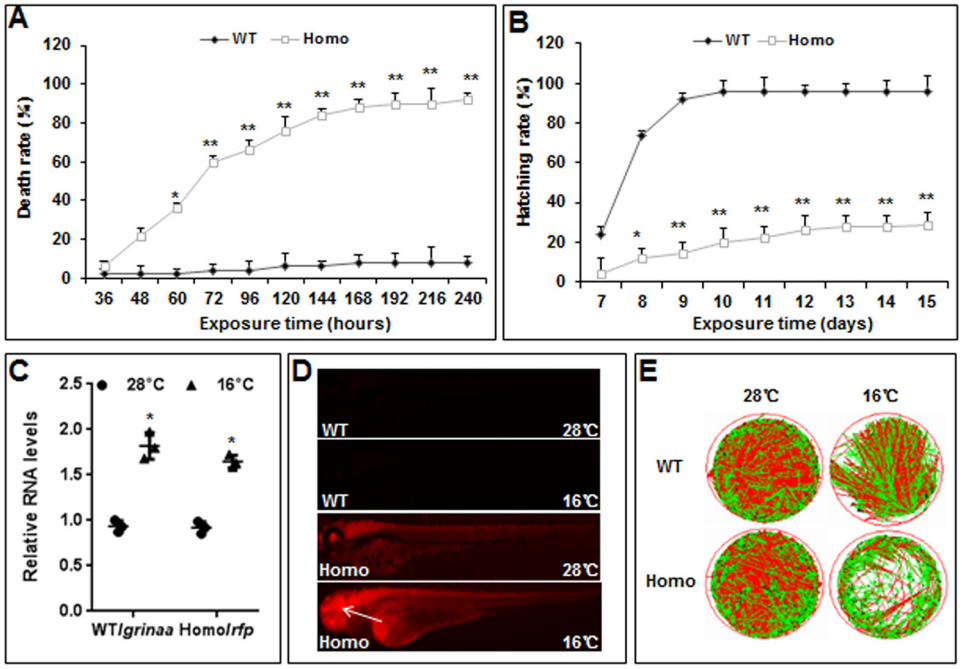

Figure 3. Effects of cold stress on zebrafish embryos. *A* and *B*, embryos at 12 hpf were exposed to 16 °C, and then death rates and hatching rates were evaluated at the indicated time points. Data are expressed as mean ± S.D. (*error bars*) ($n = 3$). *, $p < 0.05$; **, $p < 0.01$. *Homo*, homozygous. *C*, cold-induced expression of *tmbim3a*/*grinaa* or *rfp* in WT or homozygous embryos at 60 hpf was analyzed with qPCR. *, $p < 0.05$. *D*, fluorescent images of RFP expression in WT and homozygous embryos kept at 28 °C or exposed to 16 °C for 96 h. RFP fluorescence intensity reflected the expression levels of endogenous *tmbim3a*/*grinaa* in homozygous mutant embryos. *E*, swimming behaviors of WT and homozygous embryos were recorded for 2 h. *Black*, *green*, and *red colors* represent the slow, mild, and active swimming activities, respectively.

and active (*red*). In the control group at 28 °C, homozygous and WT larvae have a similar swimming activity. After exposure to 16 °C for 24 h, the swimming activity of WT larvae was slightly suppressed, but homozygous mutant larvae instantly lost their swimming ability for the first 5 min and then started to move at a mild or slow swimming activity (Fig. 3*E*). These results imply that homozygous mutant larvae exhibited a lower swimming ability than that of WT under cold stress.

Tmbim3a/Grinaa protected developing embryos from cold-induced cell death

To address cellular mechanisms underlying the roles of Tmbim3a/Grinaa in protection of embryos exposed to low temperature, phenotypic and cellular defects of developing embryos were examined. As shown in Fig. 4*A*, homozygous mutant embryos at 36 hpf were morphologically indistinguishable from the WT except for the appearance of apoptotic dots on the face of the yolk after exposure to 16 °C for 24 h. At 48 hpf, the numbers of dying cells were drastically found in the brain, spinal cord, and tail (data not shown). The ratio of homozygous mutant embryos with morphological defects (abnormal) was mostly rescued by injection of synthetic *tmbim3a*/*grinaa* capped mRNA (26.4%, injected) compared with those of uninjected (81.7%, *uninj*) and WT (0%, *WT*) controls (Fig. 4*B*). The expression of injected *tmbim3a*/*grinaa* capped mRNA was proved by Western blotting (Fig. S2*A*). However, the survival rates of WT and homozygous mutants at 16 °C were not significantly affected by injection of *tmbim3b*/*grinab*-MO (3) or *tmbim3b*/*grinab* capped mRNA (Fig. S3). These data suggest that Tmbim3a/Grinaa and Tmbim3b/Grinab have differential roles in zebrafish and that Tmbim3a/Grinaa plays a dominant role in protection of developing embryos from cold-induced cell death.

We next employed TUNEL assays to detect apoptotic cells of developing embryos of WT and *tmbim3a*/*grinaa* embryos under normal conditions and cold stress. As shown in Fig. 4*C* and Fig. S2*B*, apoptotic cells appeared in the tail region of homozygous mutants and WT embryos maintained at 28 °C and exposed to 16 °C for 60 h. There is no significant difference in apoptotic cell numbers between homozygous mutants and WT embryos at 28 °C (Fig. S2*B*); however, the number of apoptotic cells in homozygous mutants at 16 °C was significantly higher than that in the WT group (Fig. 4, *C* and *D*). Using transmission EM, we found that most of the cells in the tail of WT embryos at 16 °C maintained the integrity of the cell membrane and nucleus; however, a large number of cells in the tail of homozygous mutants demonstrated apoptotic features, including cell shrinkage, nuclear chromatin concentration, broken cell membranes, and nuclear lysis (Fig. 4*E*).

Because cold stress was reported to induce ferroptosis elsewhere (15), we next examined the involvement of ferroptosis under cold exposure by using three ferroptosis inhibitors, including the iron chelator deferoxamine (16), the MEK inhibitor U0126 (17), and the lipid peroxide scavenger Fer-1 (15). If ferroptosis occurred under cold exposure, decreased survival rates of zebrafish larvae at 16 °C could be rescued by these inhibitors. However, the survival rates of embryos at 28 and 16 °C were not significantly affected by these ferroptosis inhibitors (Fig. S4), suggesting that ferroptosis does not account for individual death of developing zebrafish embryos under cold exposure at 16 °C. Taken together, cold stress can trigger apo-

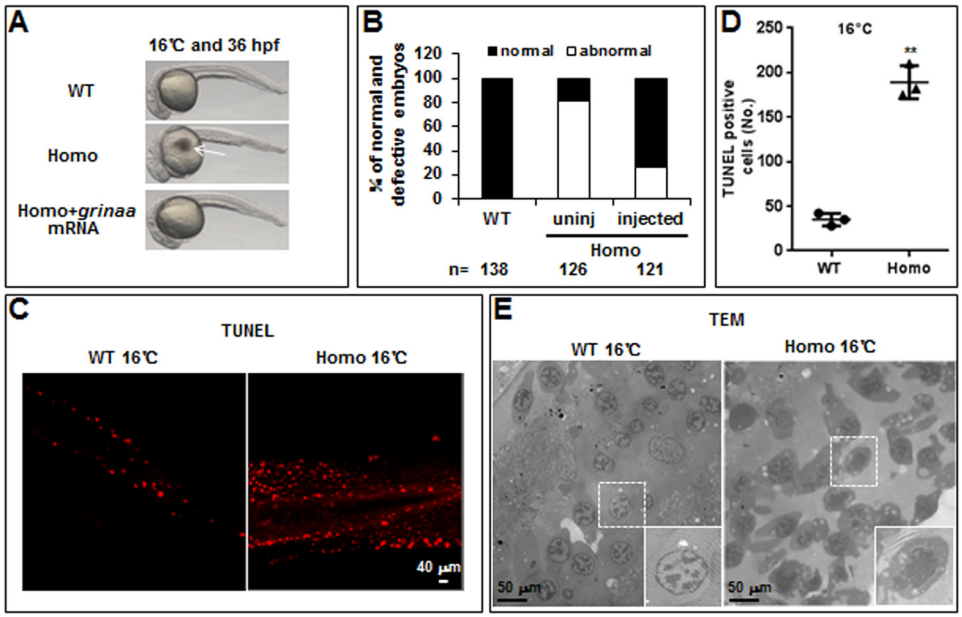

Figure 4. Cold-induced cell death can be rescued by injection of capped *Tmbim3a/grinaa* mRNA. *A*, apoptosis was detected in the yolk of homozygous (*Homo*) mutant embryos exposed to 16 °C for 36 h, but not in WT and *Tmbim3a/grinaa* mRNA-injected embryos. *B*, percentages of defective embryos. Homozygous *tmbim3a/grinaa* mutant embryos at the one-cell stage were injected with or without 600 pg of zebrafish *tmbim3a/grinaa* mRNA, followed by exposure to 16 °C for 36 h. *C*, WT and homozygous embryos were exposed to 16 °C for 60 h, fixed, and detected with TUNEL assays. *D*, statistical analysis of TUNEL-positive cells per unit area in *C*. *E*, ultrastructural changes of the yolk in WT and homozygous embryos after exposure to 16 °C for 60 h.

ptotic cell death in developing embryos and homozygous *tmbim3a/grinaa* mutants are more sensitive to cold stress than the WT.

Cold stress induced UPR-related ER stress through suppression of sarcoplasmic/ER Ca^{2+}-ATPase (SERCA) activity

Because TMBIM3/Grina is an evolutionarily conserved ER-resident protein, we examined effects of Tmbim3a/Grinaa deficiency on ER response to prolonged cold exposure by detecting the expression of UPR-related marker genes, including *atf6*, *bip*, *chop*, *edem*, and *ire1α*. qPCR analysis indicated that the transcriptional levels of these genes were significantly up-regulated in WT embryos when exposed to 16 °C *versus* 28 °C for 60 h (from 12 to 72 hpf) (Fig. 5*A*). Cold-induced expression of Chop in homozygous mutant and WT embryos was also confirmed by Western blotting (Fig. 5*B*). In addition, time course analysis revealed that the expression of these five genes was significantly induced by cold exposure during different time periods: *chop* from 12 to 18 hpf; *atf6*, *bip*, and *edem* from 12 to 24 hpf; and *irelα* from 12 to 36 hpf (Fig. 5*C*). Strikingly, the expression levels of UPR-related ER stress genes in homozygous *tmbim3a/grinaa* mutants were significantly higher than those in WT embryos after exposure to 16 °C for 60 h (from 12 to 72 hpf) (Fig. 5*D*). This suggests that cold exposure can induce an ER stress response marked by the activation of UPR pathways, and homozygous *tmbim3a/grinaa* mutants display an increased ER stress response to cold exposure.

The Ca^{2+}-ATPase of the SERCA type plays an important role in intracellular Ca^{2+} homeostasis by pumping an active Ca^{2+} efflux from the cytoplasm into the ER (18). To understand whether the activity of SERCA was affected by cold exposure, we analyzed the expression of three highly conserved genes, *atp2a1*, *atp2a2a*, and *atp2a2b*, that encode proteins of the SERCA pump (19) in zebrafish embryos. Consistent with the RNA-Seq data in our previous study (9), cold exposure at 16 °C for 60 h (from 12 to 72 hpf) led to a significant increase in the mRNA levels of the three genes in WT (Fig. 6*A*) and homozygous *tmbim3a/grinaa* mutants (Fig. S5). Despite a significant increase at mRNA levels, Ca^{2+}-ATPase activity of SERCA in developing embryos was significantly decreased after exposure to cold stress for 12–60 h (from 24 to 72 hpf) (Fig. 6*B*).

We next investigated whether the elevated activity of SERCA prevents cold-induced ER stress and apoptosis using an allosteric SERCA activator, CDN1163 (20), *versus* an inhibitor of classical ER stress (4-phenyl butyric acid (4-PBA)) (21). Similar to the treatment with thapsigargin (a specific SERCA inhibitor) at 28 °C, cold exposure at 16 °C led to a significant decrease in SERCA activity; however, CDN1163 treatment at 28 and 16 °C significantly enhanced the SERCA activity (Fig. 6*C*). The involvement of SERCA activity in the control of ER stress was shown by the fact that cold-induced *chop* expression was markedly suppressed by CDN1163 or classical ER stress inhibitor 4-PBA, but treatment with CDN1163 or 4-PBA could not abolish the cold-induced ER stress (Fig. 6*D*). We further evaluated whether inhibition of ER stress could prevent apoptosis induced by cold stress. Together with inhibited CHOP expression in (Fig. 6*D*), TUNEL assays revealed that treatment with 4-PBA or CDN1163 markedly attenuated cold-induced apoptosis (Fig. S6). Taken together, these results suggest that cold exposure inhibits the Ca^{2+}-ATPase activity of SERCA, leading to the disrupted Ca^{2} homeostasis, increased ER stress, and cell death.

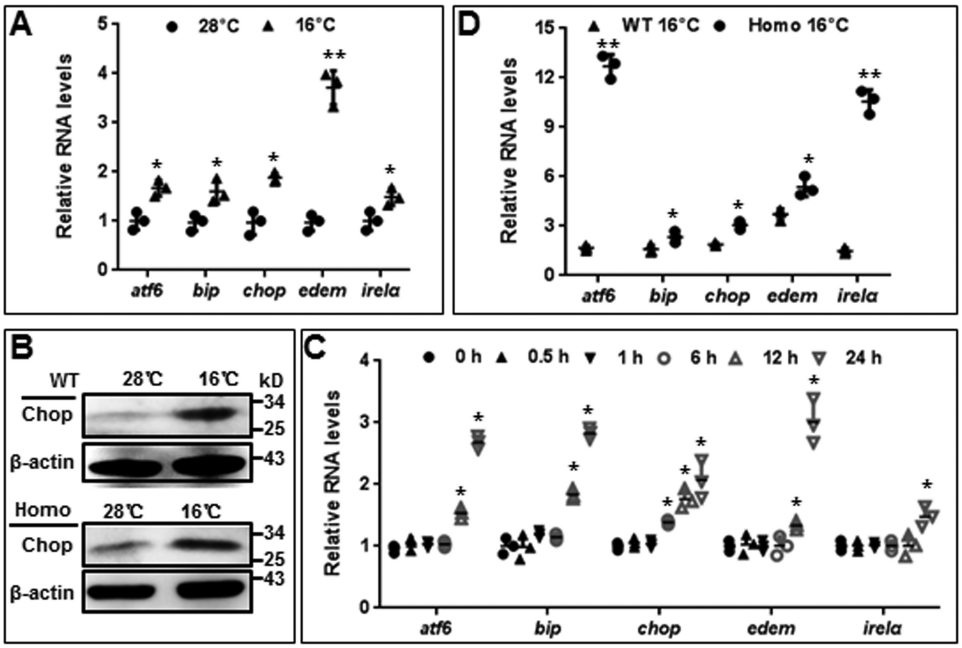

Figure 5. Cold exposure led to ER stress in developing zebrafish embryos. *A*, qPCR analysis of UPR-related genes *atf6*, *bip*, *chop*, *edem*, and *ire1α* in WT embryos after exposure to 16 °C for 60 h (from 12 to 72 hpf). The relative expression levels of these genes were normalized to that of *β*-actin gene. *B*, Western blot analysis of Chop in WT and homozygous (*Homo*) mutant embryos after exposure to 16 °C for 60 h (from 12 to 72 hpf). *β*-Actin was used as a loading control. *C*, qPCR analysis of UPR-related gene expression. WT embryos at 12 hpf were exposed to 16 °C for 0, 0.5, 1, 6, 12, and 24 h, 12–18 hpf. *D*, qPCR analysis of the expression of UPR-related genes in WT and homozygous mutants after exposure to 16 °C for 60 h (from 12 to 72 hpf).

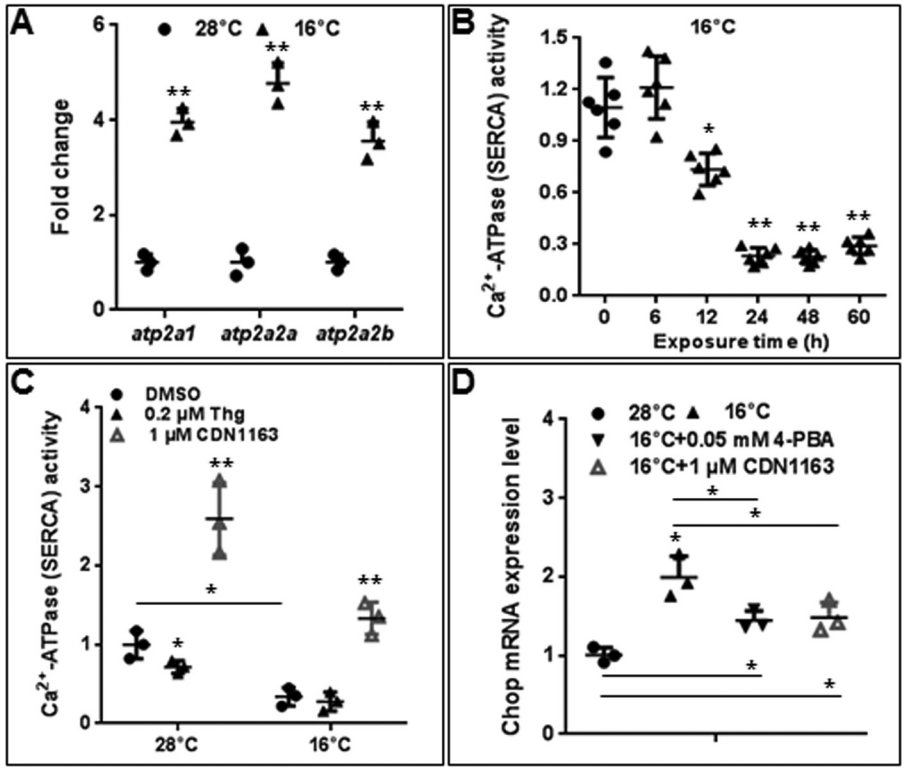

Figure 6. Cold exposure induced ER stress through suppressing the activity of SERCA. *A*, qPCR analysis of SERCA family genes *atp2a1*, *atp2a2a*, and *atp2a2b* in WT embryos exposed to 16 °C for 60 h. *Error bars*, S.D. ($n = 3$). *B*, SERCA activities of zebrafish embryos at the indicated exposure time points. Data are presented as mean ± S.D. (*error bars*) ($n = 6$), and significant differences are indicated by $p < 0.05$ (*). *C*, zebrafish embryos at 12 hpf were exposed to cold with or without 0.2 μM Thg or 1 μM CDN1163 for 60 h, and then the SERCA activity was measured. *D*, qPCR analysis of Chop mRNA levels in the indicated groups of WT embryos after exposure to 16 °C for 60 h (from 12 to 72 hpf).

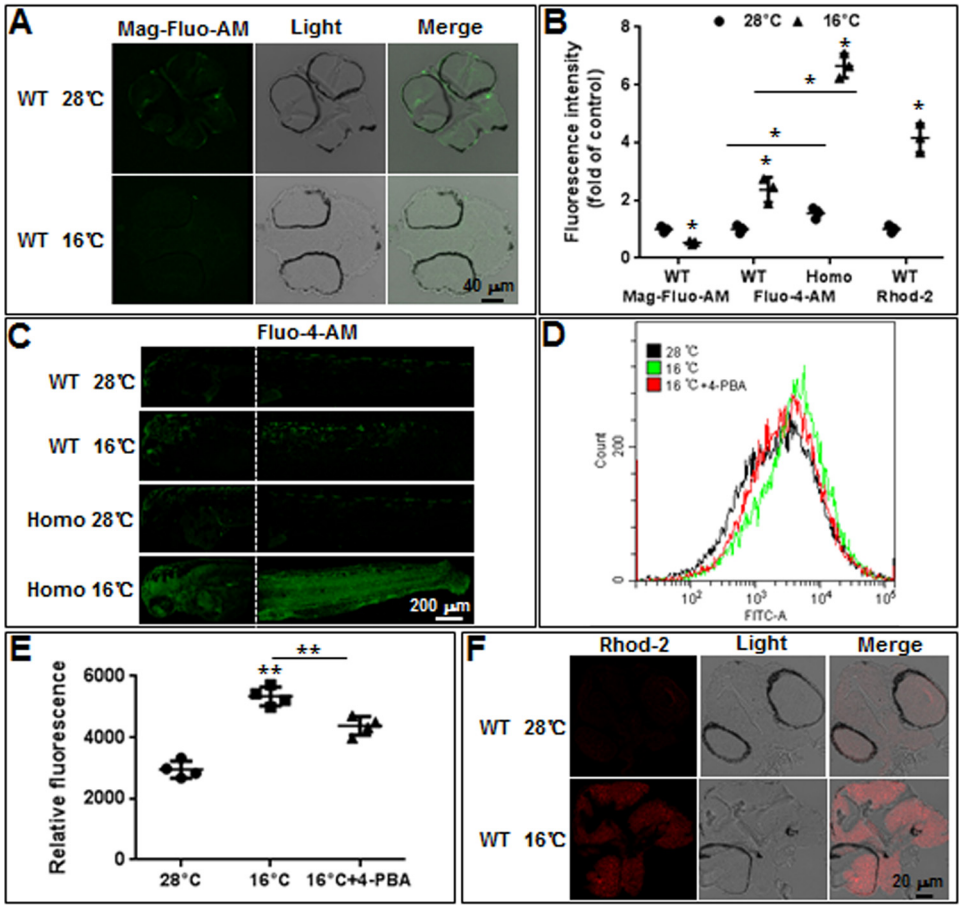

Figure 7. Cold stress stimulated ER-Ca^{2+} release and mitochondrial Ca^{2+} overload. *A*, representative confocal images of zebrafish embryo cryosections loaded with Mag-Fluo-AM. *B*, quantitative analysis of fluorescent intensities for Mag-Fluo-AM, Fluo-4-AM, and Rhod-2 by using ImageJ software. Data were expressed as mean ± S.D. (*error bars*) ($n = 3$). *, $p < 0.05$; **, $p < 0.01$ as compared with the corresponding controls. *C*, fluorescence signals were imaged in WT or homozygous (*Homo*) mutants loaded with Fluo-4-AM at 28 or 16 °C for 60 h. *D*, WT embryos were exposed to 28 or 16 °C in the presence or absence of 0.05 mM 4-PBA for 60 h, and intracellular Ca^{2+} levels were assessed by detecting Fluo-4-AM with flow cytometric analysis. *E*, statistical analysis of the FITC fluorescence in *D*. *F*, cryosections of WT embryos loaded with Rhod-2-AM at 28 or 16 °C for 60 h, followed by confocal imaging.

Cold stress disrupted Ca^{2+} homeostasis in cells of zebrafish embryos

Because ER is one of the major sites for Ca^{2+} storage in cells, we next examined the distribution of Ca^{2+} in ER of developing embryos (WT) under cold stress using a new Ca^{2+} indicator, Mag-Fluo-4-AM, a fluorescent dye to specifically monitor the distribution of Ca^{2+} in ER (22). Mag-Fluo-4-AM fluorescence intensity in WT embryos at 16 °C is markedly decreased compared with that at 28 °C, suggesting a decreased Ca^{2+} level in the ER induced by cold stress (Fig. 7, *A* and *B*). We also examined the effect of cold stress on cytoplasmic Ca^{2+} level using a specific indicator dye for cytoplasmic Ca^{2+}, Fluo-4-AM. Cold stress resulted in a significant increase of cytoplasmic Ca^{2+} in WT embryos, and strikingly, a significantly higher level of cytoplasmic Ca^{2+} was detected in homozygous *tmbim3a*/*grinaa* mutants (*Homo*) *versus* WT embryos (Fig. 7, *B* and *C*). To verify the requirement of ER stress for cold-induced Ca^{2+} release, intracellular Ca^{2+} levels were evaluated by detection of Fluo-4-AM with flow cytometric analysis. As shown in Fig. 7 (*D* and *E*), cytosolic Ca^{2+} levels markedly increased in embryos at 16 °C when compared with that of the control at 28 °C, whereas 4-PBA treatment significantly attenuated the cold-induced elevation of cytosolic Ca^{2+} levels (Fig. 7*E*). These results indicate that cold-induced ER stress led to the release of ER-Ca^{2+} from the ER into the cytoplasm, and loss of Tmbim3a/Grinaa enhanced the process of ER Ca^{2+} release.

To address whether the released Ca^{2+} from the ER could be gated into the mitochondria and finally lead to the mitochondrial Ca^{2+} overload, a mitochondrial Ca^{2+}-specific dye (Rhod-2) (22) was used to assess the changes of mitochondrial Ca^{2+} level in WT embryos at 16 and 28 °C. As shown in Fig. 7 (*B* and *F*), the Rhod-2 fluorescence intensity markedly increased in embryos at 16 °C compared with that at 28 °C, indicating that cold stress led to the increase of mitochondrial Ca^{2+} level in cells of developing embryos. Taken together, these results suggest that cold stress can stimulate the release of ER-Ca^{2+}, followed by the elevation of cytosolic Ca^{2+} level and mitochondrial Ca^{2+} overload.

Cold stress induced apoptosis through the mitochondrial death pathway

Mitochondrial Ca^{2+} overload can lead to apoptosis through the release of cytochrome *c* from the mitochondria and a collapse of mitochondrial membrane potential (MMP) (5). To address whether cold-induced ER stress causes apoptosis through this intracellular signaling pathway, effects of cold

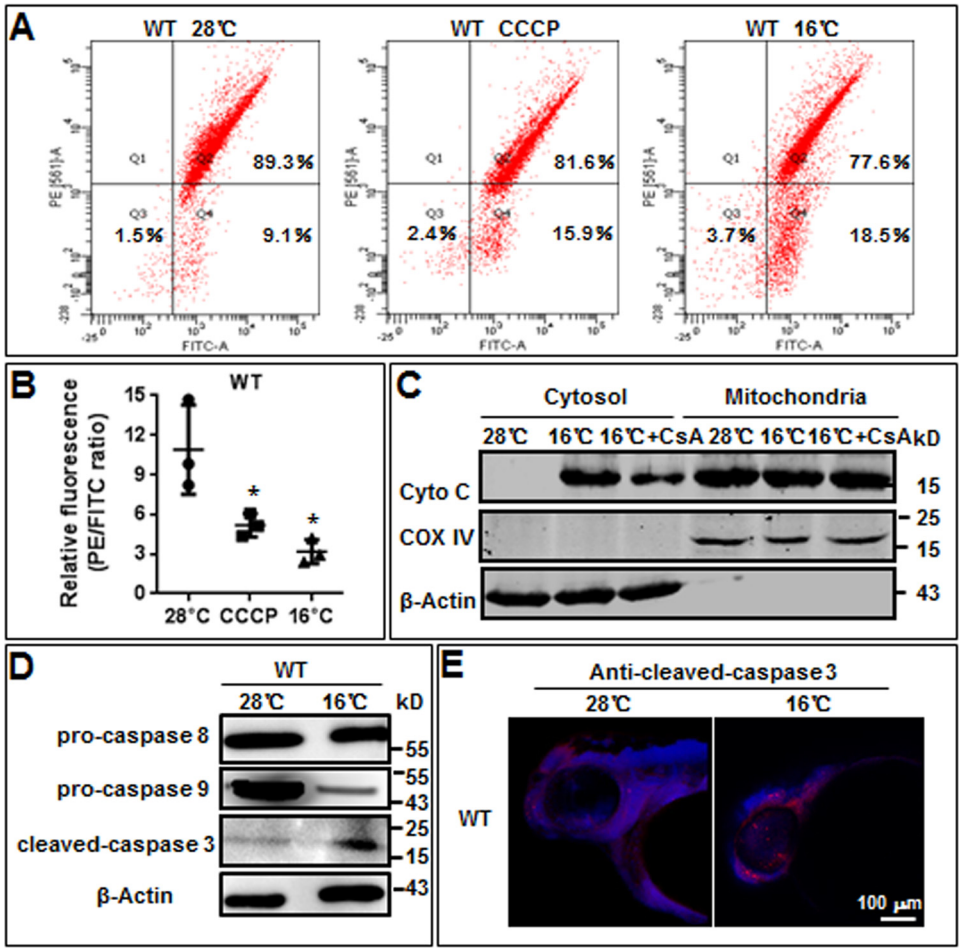

Figure 8. Cold-induced apoptosis of zebrafish embryos occurred through the mitochondria-dependent death pathway. *A*, flow cytometric analysis of mitochondrial transmembrane potential after staining with JC-1. Zebrafish WT embryos treated with 10 mM CCCP for 20 min before staining with JC-1 were used as the positive control. *B*, statistical analysis of the PE/FITC fluorescence ratios in A. *C*, Western blot analysis of the protein levels of cytochrome *c* in the cytosolic and mitochondrial fractions of zebrafish embryos. *β*-Actin was used as an internal control. *D*, Western blot analysis of signal molecules that are critical for extrinsic and intrinsic pathways of apoptosis. *E*, zebrafish WT embryos at 60 hpf were immunostained with an antibody (*red*) for active caspase-3, followed by co-staining with DAPI (*blue*).

stress on mitochondrial membrane potential were examined in zebrafish embryos with flow cytometry by detection of a fluorescent dye JC-1, which gives red fluorescence when mitochondrial membrane potential is high and green fluorescence when mitochondrial membrane potential is low (23). Carbonyl cyanide 3-chlorophenylhydrazone (CCCP), which can dissipate the mitochondrial membrane potential, was used as a positive control. We noticed that the percentage of cells showing FITC-A fluorescence markedly increased in both CCCP-treated (15.9%) and cold-treated (18.5%) groups compared with that in the control at 28 °C (9.1%) (Fig. 8*A*), and the statistical analysis of data for three independent experiments is shown in Fig. 8*B*. Similar results were found in homozygous mutants (Fig. S7, *A* and *B*). These results suggest that cold stress triggered the disruption of the mitochondrial transmembrane potential.

We next examined the effect of cold stress on intracellular localization of cytochrome *c*. As expected, Western blotting revealed that cold stress induced the release of cytochrome *c* from the mitochondria into the cytoplasm of embryonic cells. Moreover, treatment of embryos with cyclosporin A (CsA) at 5 μM, which can block an initial phase of cytochrome *c* release (24), efficiently suppressed cold-induced cytochrome *c* release in the cytosol (Fig. 8*C*).

Because the release of cytochrome *c* to the cytoplasm results in the activation of the caspase cascade (25) and caspase-3 plays a pivotal role in the execution phase of apoptosis induced by diverse stimuli (26), levels of cleaved caspase-3 (activated caspases) in WT embryos at 16 and 28 °C were detected with Western blots. As shown in Fig. 8*D*, cold stress led to an increased level of cleaved caspase-3 and a decreased level of pro-caspase-9, an initiator of intrinsic apoptosis (pro-caspase-9 cleaved and then activated caspase-3), but showed no effects on the level of caspase-8, a key mediator of extrinsic apoptosis. Moreover, immunostaining assays with an antibody for active caspase-3 indicated that cold exposure at 16 °C led to strong positive signals in the head of zebrafish embryos (Fig. 8*E*). Alternatively, we evaluated whether blockade of cytochrome *c* release could prevent cold stress–induced apoptosis. Indeed, TUNEL assays showed that CsA treatment markedly attenuated cold-induced apoptosis (Fig. S6). These results implicate that cold stress can induce apoptosis through activation of the caspase-3–dependent intrinsic apoptotic pathway.

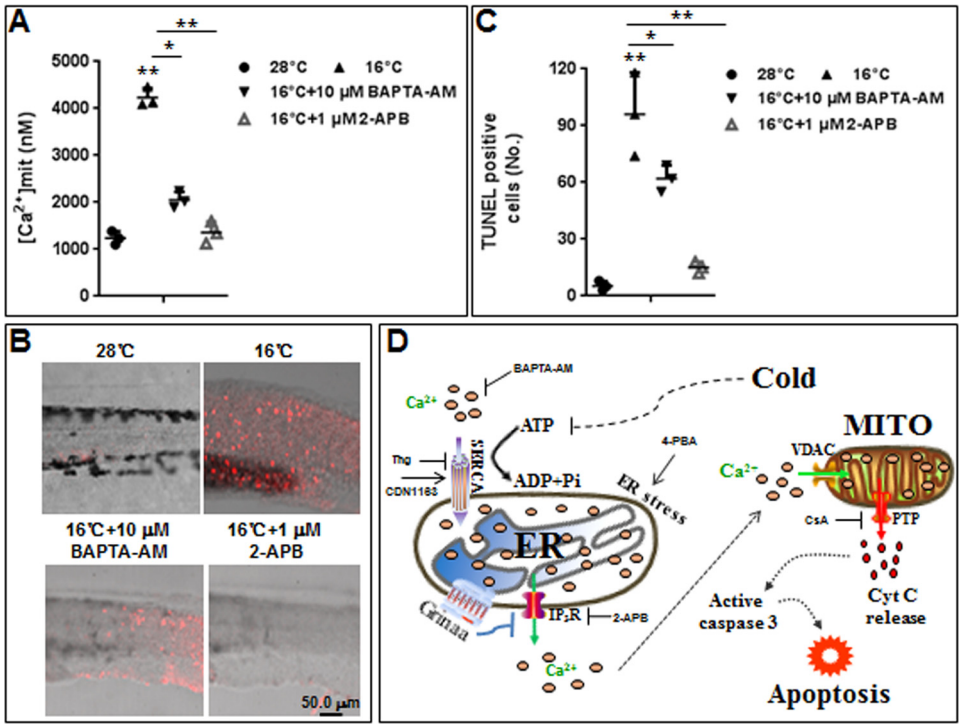

Figure 9. Treatment with cytosolic Ca^{2+} chelator (BAPTA-AM) or ER-Ca^{2+} release channel blocker (2-APB) attenuated cold-induced mitochondria Ca^{2+} elevation and apoptosis. *A*, zebrafish embryos at 12 hpf were exposed to cold with or without 10 μM BAPTA-AM or 1 μM 2-APB for 60 h, and then mitochondrial Ca^{2+} levels were measured. Data represent three independent experiments. Significant differences are indicated by $p < 0.05$ (*) and $p < 0.01$ (**) as compared with corresponding controls. *B*, embryos from *A* were fixed and assayed for apoptosis with TUNEL assays. *C*, statistical analysis of TUNEL-positive cells in *B*. Significant differences are indicated by $p < 0.05$ (*) and $p < 0.01$ (**) as compared with corresponding controls. *D*, working model for a cold-activated apoptotic pathway that involves the inhibition of SERCA activity, the release of ER-Ca^{2+} into the cytoplasm, the overload of Ca^{2+} in mitochondria (*MITO*), the release of cytochrome *c* (*Cyt C*), and the activation of caspase-3. Chemical molecules, including BAPTA-AM, Thg, CDN1163, 4-PBA, 2-APB, and CsA, were shown to control the activity of the signaling pathway.

To further examine the source of elevated mitochondrial Ca^{2+} in WT embryos under cold exposure, zebrafish embryos at 12 hpf were treated with the cytosolic Ca^{2+} chelator 1,2-bis(2-aminophenoxy)ethane-*N*,*N*,*N*′,*N*′-tetraacetate-acetoxymethyl ester (BAPTA-AM) and the ER Ca^{2+} release channel (inositol 1,4,5-trisphosphate receptor (IP_3R)) blocker 2-APB. We found that the elevated mitochondrial Ca^{2+} at 16 °C was significantly attenuated by treatment with BAPTA-AM or 2-APB in WT (Fig. 9*A*) and homozygous mutants (Fig. S7*C*). These data provide further evidence that the mitochondrial Ca^{2+} overload in embryonic cells under cold exposure mainly originated from IP_3R-mediated ER-Ca^{2+} release from the ER to cytoplasm. To address whether the elevated mitochondrial Ca^{2+} level is closely associated with cell death in embryos under cold exposure, we performed TUNEL assays in the presence or absence of BAPTA-AM or 2-APB. As shown in Fig. 9 (*B* and *C*), TUNEL-positive cells in the tail of embryos ($n = 13$) at 16 °C were significantly decreased after treatment with BAPTA-AM or 2-APB, suggesting that cold-induced embryonic cell death is rescued following inhibition of mitochondrial Ca^{2+} overload mediated by BAPTA-AM or 2-APB. Altogether, these results revealed that increased ER stress and disruption of intracellular Ca^{2+} homeostasis in *tmbim3a*/*grinaa* mutant zebrafish promote mitochondrial Ca^{2+} overload, leading to activation of the caspase-3–dependent intrinsic apoptotic pathway under prolonged cold exposure (Fig. 9*D*).

Discussion

In this study, we have generated a *tmbim3a*/*grinaa* mutant zebrafish line using a Tol2 transposon–based gene-trapping approach (12), in which the *tmbim3a*/*grinaa* expression was interrupted by the insertion of a Tol2 transposon into the second intron. Homozygous mutants are fertile and display no overt morphological phenotypes under normal rearing conditions at 28 °C. Thus, Tmbim3a/Grinaa is presumably not required for physiological regulation of embryonic development and growth in zebrafish. However, Tmbim3a/Grinaa-deficient embryos at 16 °C extensively suffered from individual death and cell death, which cannot be compensated by Tmbim3b/Grinab, suggesting a specific function of Tmbim3a/Grinaa in the protection of developing embryos against cold stress.

An increase amount of evidence suggests that TMBIM family proteins, also known as BAX inhibitor-1 (BI-1) proteins, are associated with the control of apoptosis. TMBIM1/RECS1 is an endosomal/lysosomal membrane protein that plays protective roles in Fas-mediated apoptosis by reducing Fas expression on the cell surface (27). TMBIM2/LFG is located at the plasma membrane and can prevent against cell death induced by the FAS ligand (28). TMBIM4/GAAP was found in membranes of ER and Golgi apparatus, and its overexpression can inhibit apoptosis triggered by intrinsic and extrinsic stimuli (29). TMBIM5/MICS1 resides in the inner mitochondrial mem-

brane and functions in mitochondrial morphology and cytochrome *c* release during apoptosis (30). TMBIM6 in ER membranes inhibits apoptosis and reduces histamine-induced Ca^{2+} release from intracellular Ca^{2+} stores by decreasing the efficacy of IP_3R (31). Overexpression of mouse TMBIM3/GRINA specifically inhibits cell death induced by several ER stress agents, but not by other agents that activate both intrinsic and extrinsic apoptosis (3). TMBIM3-deficient mice did not have obvious phenotypes under normal rearing condition (6), but TMBIM3/GRINA and TMBIM6 double deficiency led to lethality, and these animals are extremely susceptible to pharmacological ER stress (3), suggesting that TMBIM3/GRINA and TMBIM6 have complementary and redundant activities in the control of cell death. Similar to TMBIM3-deficient mice (6), homozygous *tmbim3a*/*grinaa* zebrafish mutants are viable and did not show any abnormal phenotypes under normal rearing conditions (Fig. 1*G*). Zebrafish Tmbim3a, which was co-localized with an ER maker, is required for the protection of embryonic cells against ER stress–associated apoptosis under prolonged cold exposure (Fig. 2*D*). However, the survival rates of WT and homozygous zebrafish embryos under cold exposure appear to not be affected by knockdown or overexpression of Tmbim3b (Fig. S3), which was co-localized with ER and Golgi markers in zebrafish cells (3). Thus, TMBIM family proteins may have evolved differential functions in the control of extrinsic and intrinsic apoptotic pathways, probably due to their differences in subcellular distributions.

ER is the central intracellular organelle that is responsible for protein translocation, protein folding, and protein post-translational modifications (32). Alterations in physiological and pathological conditions often lead to the accumulation of misfolded proteins in the ER, a process named "ER stress" that can trigger a UPR to restore protein homeostasis mainly by activation of three signaling pathways, including IRE1α, PERK, and ATF6 (33). In this study, we found that cold stress significantly induced the transcriptional expression of UPR-related marker genes, which was noticed in liver transcriptomic data of gilthead sea bream upon exposure to low temperature (11). However, little is known about functions and mechanisms of cold-induced ER stress in fish.

Ca^{2+} is an important second messenger that is involved in complex cellular functions, such as contraction, secretion, fertilization, proliferation, and metabolism (34). A large body of evidence indicates that prolonged and unregulated Ca^{2+} elevations are deleterious to a cell and can lead to apoptosis (35). It was reported that the ER-Ca^{2+} level is crucial for the control of cell fate in response to certain stimuli, such as ceramide, arachidonic acid, and oxidative stress (36), suggesting that the release of ER-Ca^{2+} is an important control point for apoptotic responses to diverse stimuli (37, 38).

Because the ER lumen is the major storage area for intracellular Ca^{2+} and Ca^{2+}-binding chaperones mediate the proper folding of proteins in the lumen of the ER (39), Ca^{2+} trafficking in and out of the ER can regulate a diversity of cellular responses and signaling transduction pathways relevant to stress response, modulation of transcriptional processes, and development (40). Several of the TMBIM family proteins can regulate ER-Ca^{2+} homeostasis by interaction with IP_3R (3, 41, 42), and TMBIM3a/Grinaa in zebrafish under cold stress likely functions through the regulation of ER-Ca^{2+} homeostasis by inhibition of IP_3R activity. Additionally, ATP-dependent SERCA plays an important role in ER calcium homeostasis (18). Indeed, we have found that cold-induced inhibition of SERCA activity is an early signal for the disruption of ER-Ca^{2+} homeostasis, because increasing the activity of SERCA can protect against cold-induced ER stress and apoptosis in zebrafish. Apoptosis acts as a response to pathogens (43) and many different intrinsic death stimuli, including growth factor deprivation, oxidative stress, DNA damage, and ER stress (44), so multiple extrinsic and intrinsic pathways of apoptosis have been identified in vertebrates. Induction of a typical extrinsic pathway of apoptosis is associated with the activation of extracellular tumor necrosis factor superfamily death receptors, followed by the recruitment of other proteins to form a complex that activates caspase-8 and caspase-3 (45). By contrast, the mitochondria plays a crucial role in the intrinsic apoptotic pathway, and the release of mitochondrial cytochrome *c* into the cytosol can lead to the formation of an apoptosome complex, which activates caspase-9 and caspase-3 (46). The mitochondrial death pathway is commonly activated in response to cell stress or damage (47). In addition, p53-mediated signaling plays important roles in the regulation of apoptosis (48, 49). However, thapsigargin-induced ER stress triggered apoptosis in zebrafish embryos independently of p53, and p63 is required for the activation of *puma* and apoptotic death that occurs 4 h after ER stress in the developing tail epidermis of zebrafish (50). In this study, we have uncovered an intrinsic apoptotic signaling pathway, including ER stress, release of ER-Ca^{2+} into the cytoplasm, disruption of cytosol Ca^{2+} homeostasis, mitochondrial Ca^{2+} overload, release of cytochrome *c*, and activation of caspase-3, which controls the cell and individual death of developing zebrafish embryos under mild and prolonged cold stress.

Taken together, the transcriptional expression of the zebrafish *tmbim3a*/*grinaa* gene in developing embryos was highly induced by cold stress. Induced expression of Tmbim3a/Grinaa can protect against cell and individual death of zebrafish under cold stress by maintaining ER-Ca^{2+} homeostasis and inhibiting the activity of the caspase-3–dependent apoptotic pathway. It will be of interest to further understand differential roles of human TMBIM/GRINA proteins in the control of apoptosis under diverse pathological conditions.

Experimental procedures

Reagents

The Ca^{2+} chelator BAPTA-AM (analytical grade) was purchased from APExBIO (Houston, TX). The 2-APB was obtained from Santa Cruz Biotechnology, Inc. (Dallas, TX). Fluo-4-AM, ER-tracker Red, and CsA were purchased from the Beyotime Institute of Biotechnology (Jiangsu, China). Inhibitors ferrostatin-1 (catalog no. 17729), deferoxamine (catalog no. 14595), and U0126 (catalog no. 70970) were obtained from Cayman. DMSO was obtained from Sigma-Aldrich. Stock solutions of all chemicals were freshly prepared in DMSO, and the final concentration of DMSO in exposure media did not exceed 0.5% (v/v).

Zebrafish strains and screening of tmbim3a/grinaa mutants

The AB strain of zebrafish was maintained in a recirculating water system, and embryos were raised according to standard procedures. Naturally fertilized embryos were staged by hpf. After co-injection of the Tol2 transposon vector pGene-Breaking (12) and *in vitro* synthesized transposase mRNA into one-cell stage fertilized eggs of zebrafish, screening of gene-trapping lines and identification of *tmbim3a*/*grinaa* mutants were carried out as described previously (51). The animal research protocol was approved by the Animal Care and Use Committee of the Institute of Hydrobiology (approval ID: Keshuizhuan 0829).

Analysis of transposon insertion site

Genomic DNAs were extracted from gene-trapping lines, and genome walking assays were performed according to the protocol of the Genome Walking Kit from TaKaRa with some modifications to obtain chromosomal DNA sequences flanking the integration sites of Tol2 transposons. Briefly, degenerate primers AP1-4 in the kit were substituted with AD5, AD6, and AD7 in our experiments (52). The PCR products were separated on the 1.5% agarose gel. Specific DNA bands were purified and cloned into pZero2/TA vector for sequencing. DNA sequences of PCR products were used for BLAST of the zebrafish genome in the ENSEMBL and NCBI database to identify insertion sites of the Tol2 transposon.

Total RNA extraction and mRNA detection

Total RNA was extracted from 30–50 developing zebrafish embryos using TRIzol reagent from Invitrogen following the manufacturer's instructions. Total RNA contents were determined by measuring the absorbance at 260 nm. The quality of RNA samples was assessed by agarose gel electrophoresis and UV spectrophotometry. First-strand cDNAs were synthesized using the First Strand cDNA Synthesis Kit from Fermentas.

qPCRs containing SYBR Green fluorescent reagent (Bio-Rad) were performed in a CFX Real-Time PCR Detection System (Bio-Rad). The relative amounts of mRNAs were calculated from the values of comparative threshold cycle (*Ct*) by using β-actin as a control. The cold stress–induced *tmbim3a*/*grinaa* expression was calculated using the $2^{-\Delta\Delta Ct}$ method. Primers used in the study were designed using the Primer Premier 5.0 software and are listed in Table S1.

WISH

Antisense and sense RNA probes were generated by *in vitro* transcription using T7 or T3 RNA polymerase and then labeled with digoxigenin (Roche Applied Science). WISH assays of zebrafish embryos were performed as described previously (52).

Immunofluorescence staining

ZF4 cells cultured in 35-mm dishes were permeabilized in Triton buffer for 3 min at room temperature, blocked for 15 min in a buffer containing 1% BSA and 0.09% sodium azide, and incubated with the antibodies. Antibodies included rabbit anti-hemagglutinin (anti-HA) (Sigma-Aldrich) and goat anti-rabbit antibody-FITC (Santa Cruz Biotechnology). 4′,6-diamidino-2-phenylindole (DAPI) was used to label the nuclei. Fluorescence images of fixed cells were acquired with a Leica SP8 confocal microscope.

Synthesis of RNA and mRNA injection

The coding sequence of zebrafish *tmbim3a*/*grinaa* gene was cloned into the vector pSBRNAX and linearized for *in vitro* transcription. Capped mRNAs were then synthesized using the mMessage Machine Kit (Ambion, Austin, TX). One-cell stage embryos were injected with the indicated doses of mRNA following the standard protocols. Then 150 injected embryos without abnormal phenotypes were selected at 12 hpf for subsequent cold-stress response assays. Phenotypes were analyzed, and survival rates were calculated after 72-h treatment.

Cold exposure

Biochemical incubators were used for temperature control and incubation of embryos. Zebrafish embryos at 12 hpf (maintained at 28 °C from fertilization) were randomly selected into dishes (50 embryos/dish) containing culture medium preconditioned at 16 or 28 °C and continued to incubate for 72 h. Then hatching, survival, and abnormal rates of zebrafish embryos were calculated, and images were taken under a stereomicroscope from Zeiss with a color CCD camera. The temperature and exposure time were determined by pre-experiments to ensure the occurrence of stress responses and reduce the mortality (13).

TUNEL assays

Zebrafish embryos at 12 hpf (maintained at 28 °C from fertilization) were exposed to 16 °C for 60 h, fixed, and subjected to TUNEL labeling. TUNEL assays were performed to detect apoptotic cells using the ApopTag® Red In Situ Apoptosis Detection Kit (Millipore, S7165).

Determination of cellular and mitochondrial Ca^{2+} levels

To monitor Ca^{2+} concentrations in the cytoplasm, mitochondria, and ER after cold exposures, zebrafish embryos were loaded with Fluo-4-AM (Beyotime, S1060), Rhod-2-AM (Genemed, GMS10153), and Mag-Fluo-4-AM (Genemed, GMS10267), respectively. Ca^{2+} levels were calculated according to the fluorescent intensity imaged under a Leica SP8 microscope. The fluorescence intensity data were then analyzed with ImageJ software to obtain the mean fluorescence intensity for histogram statistics. Mitochondrial Ca^{2+} levels were measured according to the manufacturer's instructions (Genemed, GMS10153).

MMP assays

MMP was measured by a mitochondrial membrane potential assay kit with JC-1 (Beyotime) following the manufacturer's instructions. Mean values of population fluorescence (red, aggregate form of JC-1 for normal intact MMP; green, monomeric form of JC-1 for abnormal dissipation of MMP) were measured with the flow cytometry and a FACScan system (BD Biosciences). CCCP (10 mM) was used as a positive control. The results were expressed as the ratio of red/green fluorescence

intensity. Data were analyzed using the Cell Quest (BD Biosciences) software.

Detection of Ca^{2+}-ATPase activity

The activity of SERCA was determined using a Ca^{2+}-ATPase assay kit (Nanjing Jiancheng Bioengineering Institute) following the manufacturer's instructions. The activity of SERCA in zebrafish embryos was measured with an ELISA reader at an absorbance of 636 nm.

Western blot analysis

After treatments, mutant and WT embryos (50 embryos/group) were collected and lysed in cell lysis buffer and detected with Western and IP reagents (Beyotime) containing protease inhibitor mixture (1:100), supplemented with 1 mM phenylmethylsulfonyl fluoride. Embryos were homogenized, and then embryonic lysates were centrifuged at 12,000 × *g* for 10 min at 4 °C. The supernatants were collected and quantified using the BCA Protein Assay Kit (Beyotime). After being boiled for 5 min at 100 °C in a 1× loading buffer, 20 μg of total proteins were subjected to SDS-PAGE and electrotransferred to a polyvinylidene difluoride membrane (Millipore). The membranes were blocked with 5% (w/v) dried milk in 1× TBS-Tween (TBST) overnight at 4 °C, incubated with the following antibodies and dilutions: anti-CHOP, 1:1000 (Beyotime, AC532); anti-cytochrome *c*, 1:1000 (Cell Signaling Technology, 11940); anti-caspase-8, 1:1000 (Cell Signaling Technology, 9746); anti-caspase-9, 1:1000 (Cell Signaling Technology, 9508); anti-active caspase-3, 1:1000 (BD Pharmingen, 559565); and anti-β-actin, 1:500 (Boster, BM0627). After being washed with TBST three times (5 min each time), membranes were probed with horseradish peroxidase–conjugated goat anti-rabbit or anti-mouse IgG secondary antibody at a 1:5000 dilution. Immobilon Western blotting chemiluminescence horseradish peroxidase (Millipore) acted as the substrate, and signals were observed using a Fujifilm LAS-4000 imaging system. The relative expression level of each protein was normalized with the reference protein (β-actin).

Statistical analysis

Data were expressed as means ± S.D. and analyzed with Student's *t* test to determine the significant difference ($p < 0.05$) between two treatments.

Author contributions—K. C., X. L., and T. Z. investigation; K. C. writing-original draft; X. L., G. S., Y. L., Q. L., and S. Z. methodology; S. Z. resources; Z. C. supervision; Z. C. writing-review and editing.

Acknowledgments—We thank Dr. Yan Wang (Analysis and Testing Center at the Institute of Hydrobiology, Chinese Academy of Sciences Hubei) for technical support. We are thankful to Prof. Ming Luo (University of Michigan) for critical review of the manuscript.

References

1. Danial, N. N., and Korsmeyer, S. J. (2004) Cell death: critical control points. *Cell* **116,** 205–219 CrossRef Medline
2. Strasser, A., O'Connor, L., and Dixit, V. M. (2000) Apoptosis signaling. *Annu. Rev. Biochem.* **69,** 217–245 CrossRef Medline
3. Rojas-Rivera, D., Armisén, R., Colombo, A., Martínez, G., Eguiguren, A. L., Díaz, A., Kiviluoto, S., Rodríguez, D., Patron, M., Rizzuto, R., Bultynck, G., Concha, M. L., Sierralta, J., Stutzin, A., and Hetz, C. (2012) TMBIM3/GRINA is a novel unfolded protein response (UPR) target gene that controls apoptosis through the modulation of ER calcium homeostasis. *Cell Death Differ.* **19,** 1013–1026 CrossRef Medline
4. Hu, L., Smith, T. F., and Goldberger, G. (2009) LFG: a candidate apoptosis regulatory gene family. *Apoptosis* **14,** 1255–1265 CrossRef Medline
5. Rojas-Rivera, D., and Hetz, C. (2015) TMBIM protein family: ancestral regulators of cell death. *Oncogene* **34,** 269–280 CrossRef Medline
6. Nielsen, J. A., Chambers, M. A., Romm, E., Lee, L. Y., Berndt, J. A., and Hudson, L. D. (2011) Mouse transmembrane BAX inhibitor motif 3 (Tmbim3) encodes a 38 kDa transmembrane protein expressed in the central nervous system. *Mol. Cell. Biochem.* **357,** 73–81 CrossRef Medline
7. Rauen, U., Polzar, B., Stephan, H., Mannherz, H. G., and de Groot, H. (1999) Cold-induced apoptosis in cultured hepatocytes and liver endothelial cells: mediation by reactive oxygen species. *FASEB J.* **13,** 155–168 CrossRef Medline
8. Hu, P., Liu, M., Zhang, D., Wang, J., Niu, H., Liu, Y., Wu, Z., Han, B., Zhai, W., Shen, Y., and Chen, L. (2015) Global identification of the genetic networks and cis-regulatory elements of the cold response in zebrafish. *Nucleic Acids Res.* **43,** 9198–9213 CrossRef Medline
9. Long, Y., Song, G., Yan, J., He, X., Li, Q., and Cui, Z. (2013) Transcriptomic characterization of cold acclimation in larval zebrafish. *BMC Genomics* **14,** 612–612 CrossRef Medline
10. Long, Y., Li, L., Li, Q., He, X., and Cui, Z. (2012) Transcriptomic characterization of temperature stress responses in larval zebrafish. *PLoS One* **7,** e37209 CrossRef Medline
11. Mininni, A. N., Milan, M., Ferraresso, S., Petochi, T., Di Marco, P., Marino, G., Livi, S., Romualdi, C., Bargelloni, L., and Patarnello, T. (2014) Liver transcriptome analysis in gilthead sea bream upon exposure to low temperature. *BMC Genomics* **15,** 765 CrossRef Medline
12. Clark, K. J., Balciunas, D., Pogoda, H. M., Ding, Y., Westcot, S. E., Bedell, V. M., Greenwood, T. M., Urban, M. D., Skuster, K. J., Petzold, A. M., Ni, J., Nielsen, A. L., Patowary, A., Scaria, V., Sivasubbu, S., *et al.* (2011) *In vivo* protein trapping produces a functional expression codex of the vertebrate proteome. *Nat. Methods* **8,** 506–515 CrossRef Medline
13. Long, Y., Yan, J., Song, G., Li, X., Li, X., Li, Q., and Cui, Z. (2015) Transcriptional events co-regulated by hypoxia and cold stresses in Zebrafish larvae. *BMC Genomics* **16,** 385 CrossRef Medline
14. Wang, Q., Tan, X., Jiao, S., You, F., and Zhang, P.-J. (2014) Analyzing cold tolerance mechanism in transgenic zebrafish (*Danio rerio*). *PLoS One* **9,** e102492 CrossRef Medline
15. Hattori, K., Ishikawa, H., Sakauchi, C., Takayanagi, S., Naguro, I., and Ichijo, H. (2017) Cold stress-induced ferroptosis involves the ASK1-p38 pathway. *EMBO Rep.* **18,** 2067–2078 CrossRef Medline
16. Chen, B., Yan, Y. L., Liu, C., Bo, L., Li, G. F., Wang, H., and Xu, Y. J. (2014) Therapeutic effect of deferoxamine on iron overload-induced inhibition of osteogenesis in a zebrafish model. *Calcif. Tissue Int.* **94,** 353–360 CrossRef Medline
17. Hawkins, T. A., Cavodeassi, F., Erdélyi, F., Szabó, G., and Lele, Z. (2008) The small molecule Mek1/2 inhibitor U0126 disrupts the chordamesoderm to notochord transition in zebrafish. *BMC Dev. Biol.* **8,** 42–42 CrossRef Medline
18. Higgins, E. R., Cannell, M. B., and Sneyd, J. (2006) A buffering SERCA pump in models of calcium dynamics. *Biophys. J.* **91,** 151–163 CrossRef Medline
19. Periasamy, M., and Kalyanasundaram, A. (2007) SERCA pump isoforms: their role in calcium transport and disease. *Muscle Nerve* **35,** 430–442 CrossRef Medline
20. Kang, S., Dahl, R., Hsieh, W., Shin, A., Zsebo, K. M., Buettner, C., Hajjar, R. J., and Lebeche, D. (2016) Small molecular allosteric activator of the sarco/endoplasmic reticulum Ca^{2+}-ATPase (SERCA) attenuates diabetes and metabolic disorders. *J. Biol. Chem.* **291,** 5185–5198 CrossRef Medline
21. Cai, Z., Li, F., Gong, W., Liu, W., Duan, Q., Chen, C., Ni, L., Xia, Y., Cianflone, K., Dong, N., and Wang, D. W. (2013) Endoplasmic reticulum stress participates in aortic valve calcification in hypercholesterolemic

animals. *Arterioscler. Thromb. Vasc. Biol.* **33,** 2345–2354 CrossRef Medline
22. Wang, H., Wang, Z. K., Jiao, P., Zhou, X. P., Yang, D. B., Wang, Z. Y., and Wang, L. (2015) Redistribution of subcellular calcium and its effect on apoptosis in primary cultures of rat proximal tubular cells exposed to lead. *Toxicology* **333,** 137–146 CrossRef Medline
23. Zhao, P., Han, T., Guo, J. J., Zhu, S. L., Wang, J., Ao, F., Jing, M. Z., She, Y. L., Wu, Z. H., and Ye, L. B. (2012) HCV NS4B induces apoptosis through the mitochondrial death pathway. *Virus Res.* **169,** 1–7 CrossRef Medline
24. Xu, J., Timares, L., Heilpern, C., Weng, Z., Li, C., Xu, H., Pressey, J. G., Elmets, C. A., Kopelovich, L., and Athar, M. (2010) Targeting wild-type and mutant p53 with small molecule CP-31398 blocks the growth of rhabdomyosarcoma by inducing reactive oxygen species–dependent apoptosis. *Cancer Res.* **70,** 6566–6576 CrossRef Medline
25. Lobo, G. P., Isken, A., Hoff, S., Babino, D., and von Lintig, J. (2012) BCDO2 acts as a carotenoid scavenger and gatekeeper for the mitochondrial apoptotic pathway. *Development* **139,** 2966–2977 CrossRef Medline
26. Lockshin, R. (2005) Programmed cell death: history and future of a concept. *J. Soc. Biol.* **199,** 169 CrossRef Medline
27. Shukla, S., Fujita, K., Xiao, Q., Liao, Z., Garfield, S., and Srinivasula, S. M. (2011) A shear stress responsive gene product PP1201 protects against Fas-mediated apoptosis by reducing Fas expression on the cell surface. *Apoptosis* **16,** 162–173 CrossRef Medline
28. Somia, N. V., Schmitt, M. J., Vetter, D. E., Van Antwerp, D., Heinemann, S. F., and Verma, I. M. (1999) LFG: an anti-apoptotic gene that provides protection from Fas-mediated cell death. *Proc. Natl. Acad. Sci. U.S.A.* **96,** 12667–12672 CrossRef Medline
29. Gubser, C., Bergamaschi, D., Hollinshead, M., Lu, X., van Kuppeveld, F. J. M., and Smith, G. L. (2007) A new inhibitor of apoptosis from vaccinia virus and eukaryotes. *PLOS Pathog.* **3,** e17 CrossRef Medline
30. Oka, T., Sayano, T., Tamai, S., Yokota, S., Kato, H., Fujii, G., and Mihara, K. (2008) Identification of a novel protein MICS1 that is involved in maintenance of mitochondrial morphology and apoptotic release of cytochrome *c*. *Mol. Biol. Cell* **19,** 2597–2608 CrossRef Medline
31. de Mattia, F., Gubser, C., van Dommelen, M. M. T., Visch, H. J., Distelmaier, F., Postigo, A., Luyten, T., Parys, J. B., de Smedt, H., Smith, G. L., Willems, P. H., and van Kuppeveld, F. J. (2009) Human Golgi antiapoptotic protein modulates intracellular calcium fluxes. *Mol. Biol. Cell* **20,** 3638–3645 CrossRef Medline
32. Sano, R., and Reed, J. C. (2013) ER stress-induced cell death mechanisms. *Biochim. Biophys. Acta* **1833,** 3460–3470 CrossRef Medline
33. Hetz, C., Chevet, E., and Oakes, S. A. (2015) Proteostasis control by the unfolded protein response. *Nat. Cell Biol.* **17,** 829–838 CrossRef Medline
34. Yuan, Y., Jiang, C. Y., Xu, H., Sun, Y., Hu, F. F., Bian, J. C., Liu, X. Z., Gu, J. H., and Liu, Z. P. (2013) Cadmium-induced apoptosis in primary rat cerebral cortical neurons culture is mediated by a calcium signaling pathway. *PLoS One* **8,** e64330 CrossRef Medline
35. Matsumura, H., Nirasawa, S., Kiba, A., Urasaki, N., Saitoh, H., Ito, M., Kawai-Yamada, M., Uchimiya, H., and Terauchi, R. (2003) Overexpression of Bax inhibitor suppresses the fungal elicitor-induced cell death in rice (*Oryza sativa* L.) cells. *Plant J.* **33,** 425–434 CrossRef Medline
36. Chen, Y., McMillan-Ward, E., Kong, J., Israels, S. J., and Gibson, S. B. (2008) Oxidative stress induces autophagic cell death independent of apoptosis in transformed and cancer cells. *Cell Death Differ.* **15,** 171–182 CrossRef Medline
37. Wang, S. H., Shih, Y. L., Ko, W. C., Wei, Y. H., and Shih, C. M. (2008) Cadmium-induced autophagy and apoptosis are mediated by a calcium signaling pathway. *Cell. Mol. Life Sci.* **65,** 3640–3652 CrossRef Medline
38. White, C., Li, C., Yang, J., Petrenko, N. B., Madesh, M., Thompson, C. B., and Foskett, J. K. (2005) The endoplasmic reticulum gateway to apoptosis by Bcl-X(L) modulation of the InsP3R. *Nat. Cell Biol.* **7,** 1021–1028 CrossRef Medline
39. Rizzuto, R., Pinton, P., Carrington, W., Fay, F. S., Fogarty, K. E., Lifshitz, L. M., Tuft, R. A., and Pozzan, T. (1998) Close contacts with the endoplasmic reticulum as determinants of mitochondrial Ca^{2+} responses. *Science* **280,** 1763–1766 CrossRef Medline
40. Scorrano, L., Oakes, S. A., Opferman, J. T., Cheng, E. H., Sorcinelli, M. D., Pozzan, T., and Korsmeyer, S. J. (2003) BAX and BAK regulation of endoplasmic reticulum Ca^{2+}: a control point for apoptosis. *Science* **300,** 135–139 CrossRef Medline
41. Bonneau, B., Nougarède, A., Prudent, J., Popgeorgiev, N., Peyriéras, N., Rimokh, R., and Gillet, G. (2014) The Bcl-2 homolog Nrz inhibits binding of IP3 to its receptor to control calcium signaling during zebrafish epiboly. *Sci. Signal.* **7,** ra14 CrossRef Medline
42. Chen, R., Valencia, I., Zhong, F., McColl, K. S., Roderick, H. L., Bootman, M. D., Berridge, M. J., Conway, S. J., Holmes, A. B., Mignery, G. A., Velez, P., and Distelhorst, C. W. (2004) Bcl-2 functionally interacts with inositol 1,4,5-trisphosphate receptors to regulate calcium release from the ER in response to inositol 1,4,5-trisphosphate. *J. Cell Biol.* **166,** 193–203 CrossRef Medline
43. Watanabe, N., and Lam, E. (2006) Arabidopsis Bax inhibitor-1 functions as an attenuator of biotic and abiotic types of cell death. *Plant J.* **45,** 884–894 CrossRef Medline
44. Lisbona, F., Rojas-Rivera, D., Thielen, P., Zamorano, S., Todd, D., Martinon, F., Glavic, A., Kress, C., Lin, J. H., Walter, P., Reed, J. C., Glimcher, L. H., and Hetz, C. (2009) BAX inhibitor-1 is a negative regulator of the ER stress sensor IRE1α. *Mol. Cell* **33,** 679–691 CrossRef Medline
45. Hotchkiss, R. S., and Nicholson, D. W. (2006) Apoptosis and caspases regulate death and inflammation in sepsis. *Nat. Rev. Immunol.* **6,** 813–822 CrossRef Medline
46. Elmore, S. (2007) Apoptosis: a review of programmed cell death. *Toxicol. Pathol.* **35,** 495–516 CrossRef Medline
47. Sheridan, C., and Martin, S. J. (2010) Mitochondrial fission/fusion dynamics and apoptosis. *Mitochondrion* **10,** 640–648 CrossRef Medline
48. Mei, J., Zhang, Q.-Y., Li, Z., Lin, S., and Gui, J.-F. (2008) C1q-like inhibits p53-mediated apoptosis and controls normal hematopoiesis during zebrafish embryogenesis. *Dev. Biol.* **319,** 273–284 CrossRef Medline
49. Han, R., Zhao, Q., Zong, S., Miao, S., Song, W., and Wang, L. (2016) A novel TRIM family member, Trim69, regulates zebrafish development through p53-mediated apoptosis. *Mol. Reprod. Dev.* **83,** 442–454 CrossRef Medline
50. Pyati, U. J., Gjini, E., Carbonneau, S., Lee, J. S., Guo, F., Jette, C. A., Kelsell, D. P., and Look, A. T. (2011) p63 mediates an apoptotic response to pharmacological and disease-related ER stress in the developing epidermis. *Dev. Cell* **21,** 492–505 CrossRef Medline
51. Song, G., Li, Q., Long, Y., Gu, Q., Hackett, P. B., and Cui, Z. (2012) Effective gene trapping mediated by Sleeping Beauty transposon. *PLoS One* **7,** e44123 CrossRef Medline
52. Liu, C., Song, G., Mao, L., Long, Y., Li, Q., and Cui, Z. (2015) Generation of an enhancer-trapping vector for insertional mutagenesis in zebrafish. *PLoS One* **10,** e0139612 CrossRef Medline